Transient analysis of tower-footing grounding systems with multiple inclined rods ⋆

Walter Luiz Manzi de Azevedo * **José Luciano Aslan D'Annibale** *
Anderson Ricardo Justo de Araújo * **Jaimis Sajid Leon Colqui** *
José Pissolato Filho *

* *Faculdade de Engenharia Elétrica e de Computação, UNICAMP, Campinas, SP Brasil, (e-mails: w157573@dac.unicamp.br, annibale_jose@yahoo.com.br, ajaraujo@unicamp.br; jaimis@unicamp.br; pisso@unicamp.br).*

Abstract: This paper investigates the influence of the inclination angle (in relation to the vertical axis) on the harmonic grounding impedance (HGI) of four arrangements of rods and on the performance of the Ground Potential Rise (GPR) generated on those electrodes subjected to a lightning strike. A full-wave electromagnetic software FEKO using Method of Moments (MoM) is utilized for the analysis where the soil parameters (resistivity and relative permittivity) are modeled using the recommended formulas in the CIGRÈ WG. C4.33 (2019). The analysis is carried out for three soils with low-frequency resistivities (ρ_0) of 100, 500 and 1,000 Ωm where the HGI is computed for a frequency range of 100 Hz to 10 MHz assuming the inclination angles of 0°, 15°, 30°, 45° and 60°. The transient GPR is assessed for a 1 A-0.25/100 μs lightning current. Results demonstrated that a significant reduction of the HGI is obtained when the inclination angle increases for a certain electrode arrangement. As a consequence, the transient GPR waveforms present significant mitigation for each grounding system which can be obtained only by setting distinct topology and inclination of the rods.

Keywords: transient response; lightning; ground potential rise; frequency-dependent soil; inclined grounding electrode.

1. INTRODUCTION

Tower-footing grounding system must provide a safe Ground Potential Rise (GPR) to protect people near the hit tower structure subjected to a lightning strike during the transient state. Besides that, these grounding electrodes must guarantee a low impedance path for high currents to disperse in the soil. A low impedance path decreases the number of outages in power systems due to backflashover over the insulator string, and reduce the induced voltages that may damage installations and equipment caused by these fast-front phenomena (Grcev, 2008). Generally, the tower-footing grounding systems are composed of metallic conductors buried vertically or horizontally in the soil. In order to obtain a low tower-footing grounding impedance, different electrode arrangements can be used which occupies a considerable area around the tower structure or installed in a deep burial depth (Batista et al., 2021).

In low resistivity soils, short rods are commonly employed for grounding. However, in moderate- and high-resistive soils, long electrodes are connected to the tower feet, so-called counterpoise electrodes. Additionally, for the transmission towers located on uneven terrains, urban areas or due to environmental requirements, its tower-footing grounding system must be limited to a reduced area. On this frame, arrangements with multiple inclined electrodes can be an interesting alternative to overcome these issues to obtain a low impedance in the grounding system (Grcev et al., 2021).

In the literature, tower-footing grounding impedance can be represented by: (i) a static resistance R_{dc} which is a good approximation for slow-front disturbances, such as faults, whose frequency wide-band varies from dc to tens of kHz or steady state analysis; (ii) harmonic grounding impedance (HGI) $Z(j\omega)$, depending only on the geometry and electrical parameters of the conductors and soil, being valid for a frequency range from dc up to the highest frequency in the spectrum of the disturbance; (iii) impulse impedance Z_p which is a concise representation resulting from the time-shift between the developed GPR and the injected current (Visacro, 2018). Additionally, the frequency dependence of soil electrical parameters (resistivity and permittivity), water content and ionization effect must be included to properly represent the ground for the transient analysis (CIGRE C4.33, 2019).

This paper studies the influence of the inclination angle on four arrangements consisting of 1, 2 3 and 4 rods buried in homogeneous soils. For this analysis, the HGI is calculated over a large frequency content and the lightning performance of the GPR developed for an impulsive current in each grounding system is investigated. A full-

⋆ This work was supported by the Coordenação de Aperfeiçoamento de Pessoal de Nível Superior (CAPES)—Finance code 001 and by São Paulo Research Foundation (FAPESP) (grants: 2019/01396-1 and 2021/06157-5).

wave electromagnetic software FEKO computes the HGI using the Method of Moments (MoM) for a frequency range of 100 Hz to 10 MHz, assuming that frequency-dependent electrical soil parameters (resistivity and permittivity) are modeled by the recommended formulas in CIGRÈ WG C4.33 (2019) (CIGRE C4.33, 2019). The arrangements are buried in three distinct soils with low-frequency resistivities (ρ_0) of 100, 500 and 1,000 Ωm where the inclination angles of 0°, 15°, 30°, 45° and 60° are considered. The time-domain responses (GPR) are evaluated for a 1A,0.25/100 μs lightning subsequent return stroke. Results have demonstrated that a significant reduction in the HGI is obtained when the inclination angle increases and also when more conductors are added to the grounding system. The GPR waveform presents a pronounced reduction, especially at its peak value, in each electrode arrangement which can be obtained in any topology using distinct inclination angles in relation to the vertical axis.

2. METHODOLOGY

In this work, the HGI $Z(j\omega)$ of four distinct arrangements of grounding electrodes were calculated using the electromagnetic simulation software FEKO ™(FEKO, 2018). For this purpose, the soil electrical parameters resistivity $\rho_s(f)$ and permittivity $\epsilon_r(f)$ must be properly represented for the computation of the HGI. In the literature, various authors have proposed different models based on several measurements carried out in field or laboratory. The recommended expressions by CIGRÈ WG. C4.33 (2019) to calculate the frequency-dependent resistivity $\rho_s(f)$ and relative permittivity $\varepsilon_r(f)$ are given by (CIGRE C4.33, 2019)

$$\rho_{\mathrm{s}}(f) = \rho_0 \left[1 + 4.7 \times 10^{-6} \rho_0^{0.73} f^{0.54}\right]^{-1}, \quad (1)$$

$$\varepsilon_{\mathrm{r}}(f) = 12 + 9.5 \times 10^{4} \rho_0^{-0.27} f^{-0.46}, \quad (2)$$

where ρ_0 [Ω.m] is the low-frequency resistivity measured at 100 Hz.

The procedure to compute the HGI $Z(j\omega)$ in the electromagnetic software FEKO is described in the following steps:

(1) Construction of the grounding system and the delimitation of the domain (ground) in the CAD-FEKO using available geometric solids and lines (Figure 1);
(2) Definition of the medium (homogeneous soil) with its electrical parameters (resistivity, permittivity and permeability) and the arrangement of the grounding electrodes (inclined rods) in the simulation domain (Figure 1);
(3) Set a Perfect Electric Conductor (PEC) surface on the top of the grounding system buried into the characterized soil.
(4) An electric *port*, defined as an excitation voltage source $V_S(j\omega) = 1\angle 0°$ V, is inserted at the top of the arrangement , as detailed in Figure 1;
(5) Select the frequency range for the simulation. The grounding system is discretized (meshes) whose size of each element is related to the wavelength (λ) and the maximum frequency (f_{max});
(6) Calculation of the induced current $I_t(j\omega)$ into the metallic array using MoM based on the integral equations (from Maxwell's equations) applied to the structure buried in a homogeneous media over the selected frequency range. Details of the modeling of the scattering electric field using MoM can be found in (Usanos et al., 2014)
(7) The harmonic impedance of the grounding system is given by the ratio of

$$Z(j\omega) = \frac{V_S(j\omega)}{I_t(j\omega)}. \quad (3)$$

where $V_S(j\omega)$ is the grounding electrode voltage and $I_t(j\omega)$ is the calculated injected current into the grounding system by FEKO/MoM.

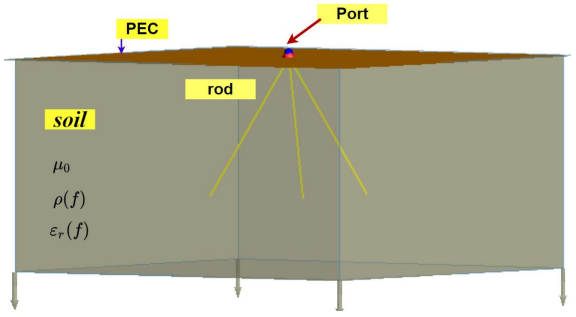

Figure 1. Simulation domain in FEKO with a 3-rod system.

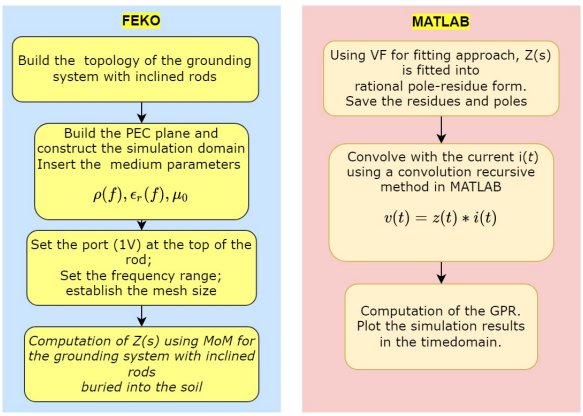

Figure 2. Steps to compute transient GPRs for the inclined rods.

The HGI $Z(j\omega)$ is approximated by a function $Z_{fit}(s)$ composed of the sum of rational functions with an independent and a frequency-dependent terms, expressed by (Gustavsen and Semlyen, 1999)

$$Z(s) \approx Z_{fit}(s) = \sum_{k=1}^{n} \left(\frac{c_k}{s + a_k}\right) + d + bs, \quad (4)$$

where c_k are the residues, a_k are the poles that can be real or complex conjugate pairs and n is the number of poles for the rational function synthesis. The terms d and b are real constants, and $s{=}j\omega$ is the complex frequency (Gustavsen and Semlyen, 1999). The transient GPR $v(t)$ developed for a certain injected current $i(t)$, from a remote point, is given as follows

$$v(t) = \mathcal{L}^{-1}\left\{Z(s) \times \mathcal{L}\left\{i(t)\right\}\right\} = z(t) * i(t) \quad (5)$$

where $\mathcal{L}$ is the Laplace transform and (*) stands for the convolution between the two functions. The numerical solution of (5) is given by (Colqui et al., 2021)

$$v(t) = \alpha v(t - \Delta t) + \beta i(t) + \mu i(t - \Delta t), \qquad (6)$$

where coefficients α, β and μ are derived assuming that the injected $i(t)$ is linear in the small time-step Δt detailed in (Colqui et al., 2021). The steps to obtain $Z(j\omega)$ and the GPR are summarized in Figure 2.

3. NUMERICAL RESULTS

Numerical results have been divided into the following sections. In section 3.1, the validation of the proposed topology in FEKO is presented. In section 3.2, the computed HGI and the developed GPR waveforms are analyzed.

3.1 Validation of the proposed topology

To validate the topology proposed in FEKO using MoM, the HGI of rods are calculated for the following conditions: two rods of 3 m and 30 m in length and radius of 7 mm, buried in a homogeneous soil with resistivity of 3,000 Ω.m and relative permittivity of ε_r of 10. The HGI are calculated for a frequency range of 100 Hz to 5 MHz and the obtained results are compared with those computed in (Grcev et al., 2018), assumed in this work as the reference. The HGI (magnitude and phase) is illustrated in Figure 3-a and -b, respectively. As seen in these figures, the HGI of the two rods computed with the proposed topology in FEKO using MoM is in excellent agreement with those computed with by (Grcev et al., 2018) for the same frequency range. As expected, longer rod will result into a small value of impedance at low frequencies. However, above a certain frequency, the inductive or capacitive behaviour will predominate depending on the frequency range. In addition, the transient GPR developed for a certain lightning strike is computed for each rod. For this purpose, the injected lightning current is modeled

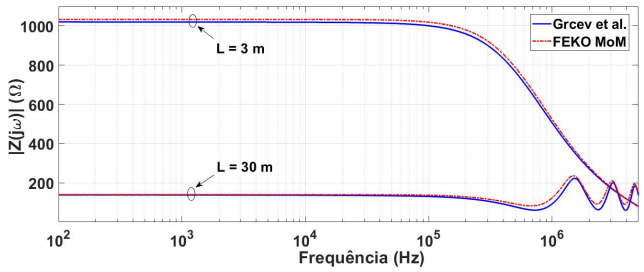

(a)

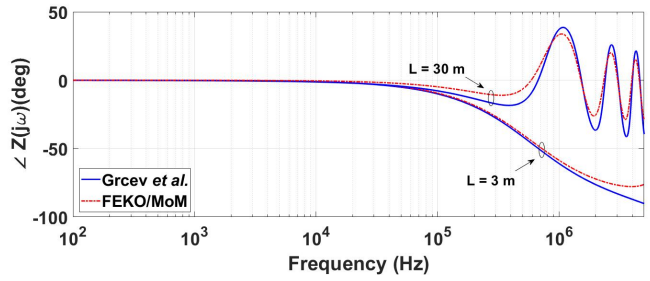

(b)

Figure 3. Comparison for HGI of 3 and 30-m rods between FEKO/MoM and (Grcev et al., 2018): (a) Magnitude; (b) Phase.

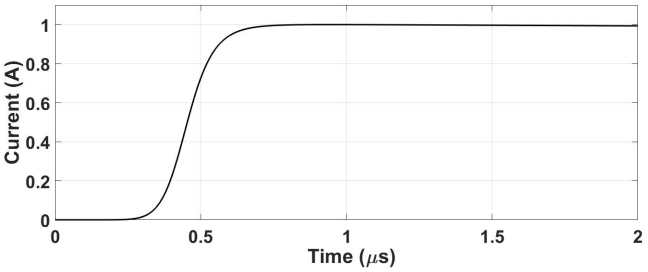

(a)

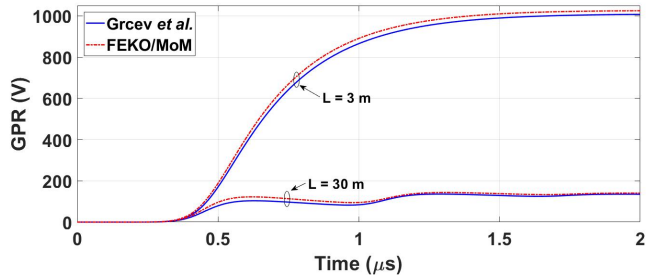

(b)

Figure 4. (a) Normalized lightning current of 1 A,0.25/100 μs; (b) Comparison for the GPR developed for the subsequent return stroke obtained with FEKO/MoM and (Grcev et al., 2018)

by subsequent return stroke described by the Heidler's expression, given by (Aniserowicz, 2020)

$$I_p(t) = \frac{I_0}{\eta} \frac{(t/\tau_1)^n}{1 + (t/\tau_1)^n} e^{-t/\tau_2}, \qquad (7a)$$

$$\eta = \exp\left[-\frac{\tau_1}{\tau_2} \left(n \frac{\tau_2}{\tau_1} \right)^{1/n} \right], \qquad (7b)$$

where I_0 [A] is the lightning amplitude, τ_1 [s] and τ_2 [s] are the front and the decay time constants, respectively. The n is an integer coefficient and η is a correction factor for the current peak. The lightning current parameters are I_0 = 50 kA, $\tau_1 = 0.454$ μs, $\tau_2 = 143$ μs, $n = 10$ and $\eta = 0.993$. The lightning current waveform is plotted in Figure 4-a. The developed GPR for the two rods using the lightning current in (7) are shown in Figure 4-b.

It can be seen that for both GPR waveforms, the results obtained with FEKO have presented an excellent agreement in the time-domain responses. The simulation domain presented here has provided a accurate modeling in the large frequency range covering up the frequency content (dc to few MHz) related to fast-front disturbances (lightning) hitting the power system.

3.2 Lightning performance of topologies with inclined rods

The four distinct arrangements are illustrated in Figure 5, named from T_1 to T_4,according with the number of rods. The inclination angle α is measured from the vertical z-axis for each rod of the arrangement as detailed in Figure 5-(e). Each rod has a length of 30 m and a radius of 12.5 mm and the grounding systems are buried in three distinct homogeneous soils. The soil is modeled by its frequency-dependent electrical parameters (resistivity and relative permittivity) represented by recommended approach detailed in (CIGRE C4.33, 2019) given by (1)

Table 1. Impulse impedance Z_p (Ω) for each topology.

	100 Ω.m				500 Ω.m				1,000 Ω.m			
α	T_1	T_2	T_3	T_4	T_1	T_2	T_3	T_4	T_1	T_2	T_3	T_4
0°	20.3	20.3	20.3	20.3	38	38.5	38.5	38.5	47.3	47.3	47.3	47.3
15 °	20.2	12.9	10.3	9.0	38.4	24.0	18.8	16.3	47.1	29.2	22.7	19.7
30 °	20.1	11.7	8.7	7.3	37.8	21.7	16.0	13.3	46.4	26.5	19.5	16.1
45 °	19.2	10.7	7.6	6.2	36.7	20.0	14.2	11.4	45.1	24.5	17.3	13.8
60 °	18.2	9.7	6.7	5.3	34.9	18.3	12.6	9.8	42.9	22.4	15.4	11.9

and (2). In this study, soils with low-frequency resistivity (ρ_0) of 100, 500 and 1,000 Ω.m are considered. The inclination angles of 0°, 15°, 30°, 45° and 60° were adopted for all arrangements. Additionally, for practical analysis, the GPR is calculated assuming that the injected current is normalized and the time step Δt of 100 μs.

The HGI and the developed GPR for the subsequent return stroke $i(t)$ in (7) considering several angle α for the topology T_1 is illustrated in Figure 6. As can be seen in this figure, the angle α does not have an notable impact on the HGI for low-resistivity soils of 100 and 500 Ω.m. However, a slightly difference can be seen at the HGI along the frequency range. In relation to the developed GPR waveforms, these differences in the peak values for the time-domain response can be small for the low-frequency soils. However, this peak difference increases for high-resistivity soils, as observed in Table 1. Considering the topology T_2, the HGI and the developed GPR are illustrated in Figure 7. It can be noted in this figure that the inclination angle has a great impact on the HGI, and consequently, on the developed GPR. As depicted, the impedance at low frequencies (between 100 Hz and 1 kHz), so-called low-frequency or static resistance R_{dc}, decreases as the inclination angle increases. Above a certain frequency, the inductive or capacitive behaviour becomes predominant. Furthermore, the R_{dc} is proportional to the low-frequency soil resistivity ρ_0.

Concerning the GPR waveforms, the GPR is significantly reduced as the inclination angle increases, being a consequence of the smaller HGI for a certain soil resistivity. The peak values of GPR for the topology T_2 are organized in Table 1 for all soil resistivities. For the topology T_3, the HGI and the developed GPR are depicted in Figure 9. As shown in these figures, at low frequencies, the static resistance is lower in comparison with those computed with two electrodes in the topology T_2. On the other hand, at high frequencies, the value of HGI will be depended on the soil parameters and the mutual coupling of electrodes in the arrangement. The transient GPR developed for the subsequent current has presented a pronounced reduction when the 3-rod topology is considered. This reduction is clearly seen in Table 1. Finally, the HGI for the topology

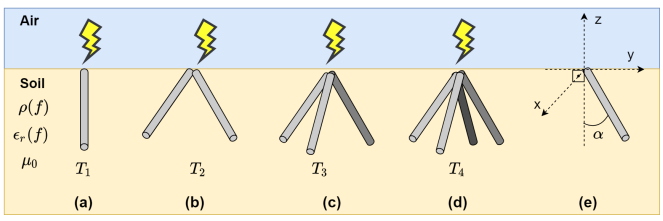

Figure 5. Arrangements for inclined rods studied: (a) T_1; (b) T_2; (c) T_3; (d) T_4; (e) Inclination angle α.

T_3 is depicted in Figure 8. As depicted in this figure, the lowest value of the static resistance is obtained when the 4-rod topology is utilized for the simulations. As a consequence of the low HGI, the developed transient GPR waveforms have presented the lowest values in comparison with those calculated for the previous topologies. This fact can be confirmed in Table 1 for the peak values of the GPR. As a general observation, one can note that as the inclination angle increases, the peak value of the GPR decreases for a certain topology.

In lightning performance studies, either in EMT-type programs or in practical engineering analysis, the tower-footing grounding impedance can be usually represented by the impulse impedance (Visacro, 2018). The impulse impedance is given by (Grcev, 2008)

$$Z_p = \frac{\max\left[GPR\right]}{\max\left[i(t)\right]} = \frac{V_P}{I_P}, \tag{8}$$

where V_p and I_p are the peaks of the developed GPR and injected lightning current, respectively. In this work, the peak of the lightning current is equal to 1 A. The calculated impulse impedance (or voltage peak) for each topology is organized in Table 1. It can be seen from this table that as the inclination angle increases, the values of Z_p decrease significantly for each electrode arrangement. Moreover, the Z_p increases with the increasing soil resistivity and the variation of Z_p is more pronounced when more conductors are used in the arrangement. Then, adding inclined electrodes in a certain arrangement of grounding system configures an interesting alternative to achieve low impedance to dissipate high currents into the soil when transmission towers are subjected to lightning strikes.

To investigate the influence of the inclination angle α on the performance of transient GPR, two types of parameters are employed in this analysis: First, the percentage reduction $\delta(\%)$ of peak values between distinct topologies concerning the 1-rod configuration T_1, given as follows

$$\delta(\%) = \frac{V_p(T_1) - V_p(T_j)}{V_p(T_1)} \times 100\%, \tag{9}$$

where $V_p(T_1)$ and $V_p(T_j)$ are the voltage peaks obtained for the topology T_1 and T_j, for j-rod topology, (j = 2, 3, 4) respectively, assuming that the inclination angle α is constant. The voltage peaks (in V) and percentage variation $\delta(\%)$ for each case is organized in Table 2. It can be seen in this table that when $\alpha = 0°$, the parameter δ has no variation since the software FEKO interprets each arrangement (T_2, T_3 and T_4) as a topology composed of 1 single rod. However, when the number of rods increases, one notes that the variation δ gets higher for a constant inclination angle.

Additionally, when the soil resistivity increases, the values of δ have no significant variation assuming a constant angle

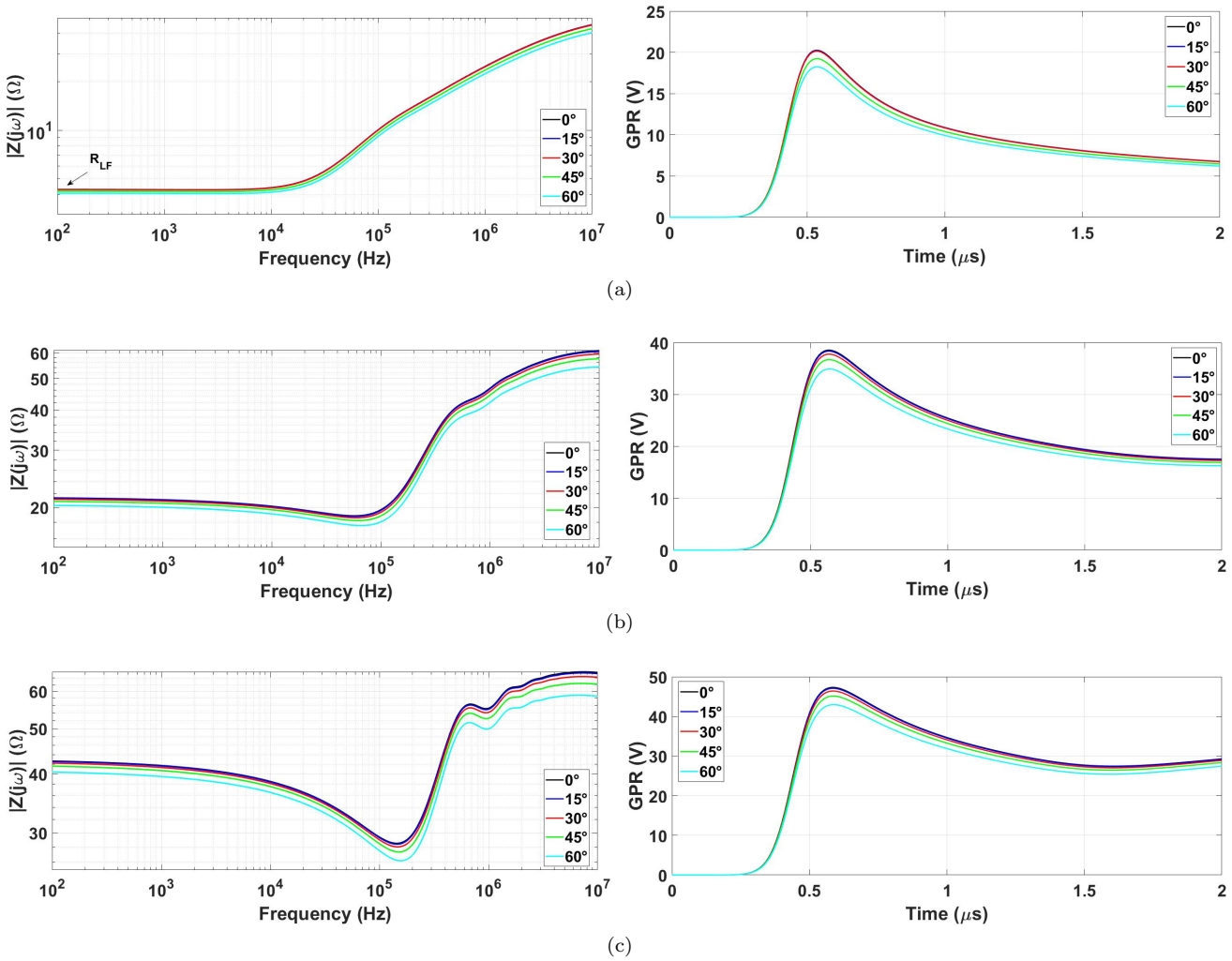

Figure 6. HGI (left) and developed GPR (right) for the topology T_1: (a) 100 Ω.m; (b) 500 Ω.m; (c) 1,000 Ω.m

Table 2. Percentage variation $\delta(\%)$ in relation to each topology in relation to T_1.

	ρ = 100 Ω.m			ρ=500 Ω.m			ρ=1,000 Ω		
α	T_2	T_3	T_4	T_2	T_3	T_4	T_2	T_3	T_4
15 °	36	49	56	38	51	58	38	38	58
30 °	42	57	64	43	58	65	43	58	65
45 °	44	60	68	46	61	69	46	62	69
60 °	47	63	71	48	64	72	48	64	72

for the studied grounds. Taking the scenario with 2-rod topology T_2, the calculated has δ of 36%, 38% and 38% for the soils of 100, 500 and 1,000 Ω.m, respectively. As expected, the 4-rod topology T_4 has presented the highest values of δ for all soil resistivities, reaching the maximum when the inclination angle $\alpha = 60°$ is assumed. In this scenario, one sees a significant variation (around 70%) in the peak values of the transient GPR for 3 soils studied. The results have demonstrated that using arrangement with multiple inclined rods offers, a good reduction in the time-domain voltages compared with those responses computed with a single rod.

The second type of parameter is the percentage reduction $\Delta(\%)$ related to the variation of the inclination angle α, in relation to 0°. assuming a fixed topology. The $\Delta(\%)$ is calculated by

$$\Delta(\%) = \frac{V_p(\alpha = 0°) - V_p(\alpha_j)}{V_p(\alpha = 0°)} \times 100\%, \qquad (10)$$

where $V_p(\alpha = 0°)$ and $V_p(\alpha)$ are the voltage peaks of the transient GPR waveforms calculated for $\alpha = 0°$ and other angles $\alpha_j = 15°$, 30°, 45 ° and 60°, respectively. The percentage variation $\Delta(\%)$ for each case is depicted in Table 3. This table shows that as the inclination angle α gets higher, the reduction in the peak values of the GPR increase. It is noted that a pronounced reduction effect occurs when an arrangement with multiple conductors is employed as a tower-footing grounding system.

As an example, in the scenario with the 4-rod topology using an inclination angle of 60°, the obtained peak voltages are reduced (approximately) by 75% considering the 3 types of grounds studied in this work. However, for a 1-rod topology T_1, the reductions seen in the GPR peaks are lower than 10.3% and 9.3% for the soils of 100 and 1,000 Ω.m, respectively, which results in a low impact on the generated potential for this fast-front current. The variation of the inclination angle can result in a significant impact on the developed potential which must be below a safe limit to protect people and avoid damages to the electrical installations nearby the hit transmission tower.

Table 3. Percentage variation $\Delta(\%)$ for the angle α.

	100 Ω.m				500 Ω.m				1,000 Ω.m			
α	T_1	T_2	T_3	T_4	T_1	T_2	T_3	T_4	T_1	T_2	T_3	T_4
15 °	0.5	36.5	49.3	55.7	0.3	37.7	51.2	57.7	0.4	38.3	52.0	58.4
30 °	1.0	42.4	57.1	64.0	1.8	43.6	58.4	65.5	1.9	44.0	58.8	66.0
45 °	5.4	47.3	62.6	69.5	4.7	48.1	63.1	70.4	4.7	48.2	63.4	70.8
60 °	10.3	52.2	67.0	73.9	9.4	52.5	67.3	74.5	9.3	52.6	67.4	74.8

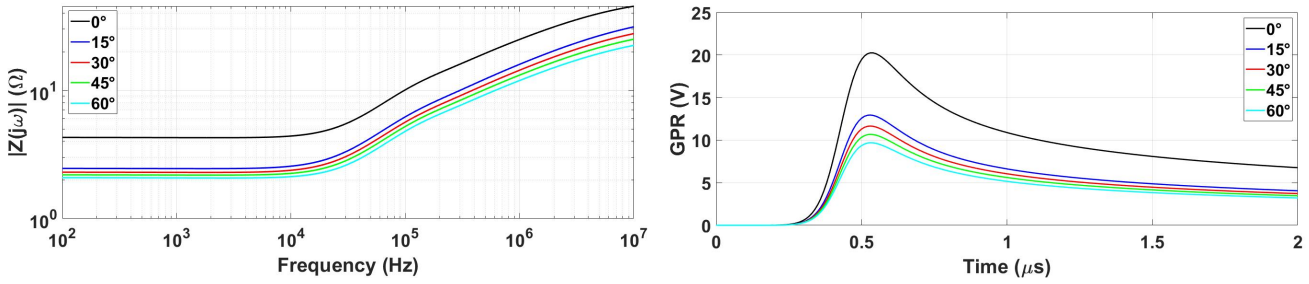

(a)

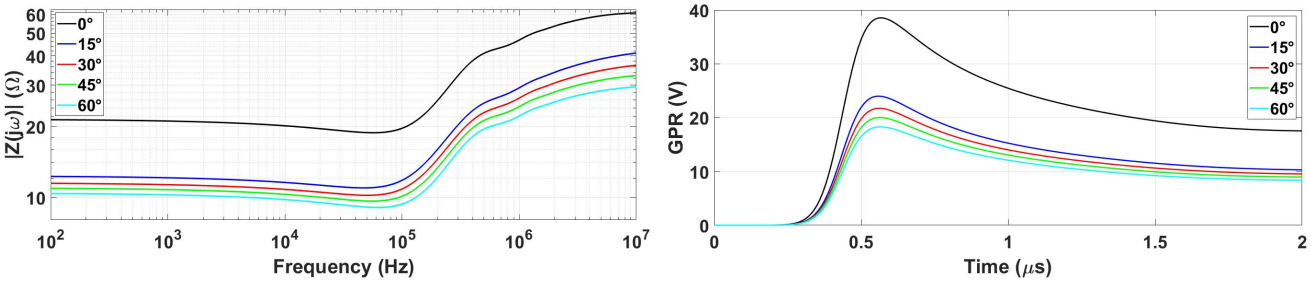

(b)

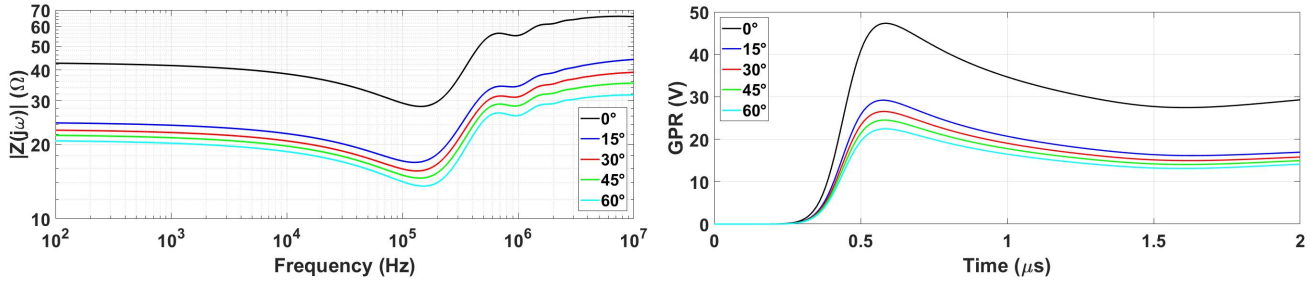

(c)

Figure 7. HGI (left) and developed GPR (right) for the topology T_2: (a) 100 Ω.m; (b) 500 Ω.m; (c) 1,000 Ω.m

4. CONCLUSIONS

This paper analyzed the influence of the inclination angle on the four arrangements with distinct inclined rods buried in frequency-dependent homogeneous soils and its impact on the lightning performance in the time domain responses.

The HGI was calculated over a frequency range of 100 Hz to 10 MHz, employing a proposed simulation domain in a full-wave electromagnetic solver using MoM. Results have shown an excellent performance for the proposed simulation domain in the electromagnetic solver compared to the harmonic impedance computed with a rigorous model available in the literature. The HGI was assessed for the electrode arrangements buried in homogeneous frequency-dependent soils whose resistivity and permittivity was represented by recommended expressions in the brochure CIGRÈ WG C4.33 (2019). The arrangements were buried in three distinct soils with low-frequency resistivities of low, moderate and high resistivity. Four inclination angles were assumed: (0°, 15°, 30°, 45° and 60°). Results have indicated that the static resistance at low frequencies decreases with the increasing inclination angle or the number of inclined rods in the arrangement. However, the HGI may assume either inductive or capacitive behaviour above a certain frequency, where each behaviour will depend on the frequency range, the electrode arrangement and soil parameters (resistivity and permittivity). The transient responses developed for a lightning subsequent return stroke have demonstrated that a pronounced reduction on the HGI will have a major impact on the GPR waveforms, especially at its peak values which are lower in comparison with those computed with 1-rod topology. The highest reduction were obtained for the angle of 60°. It is shown in this work that for a certain electrode arrangement, safe

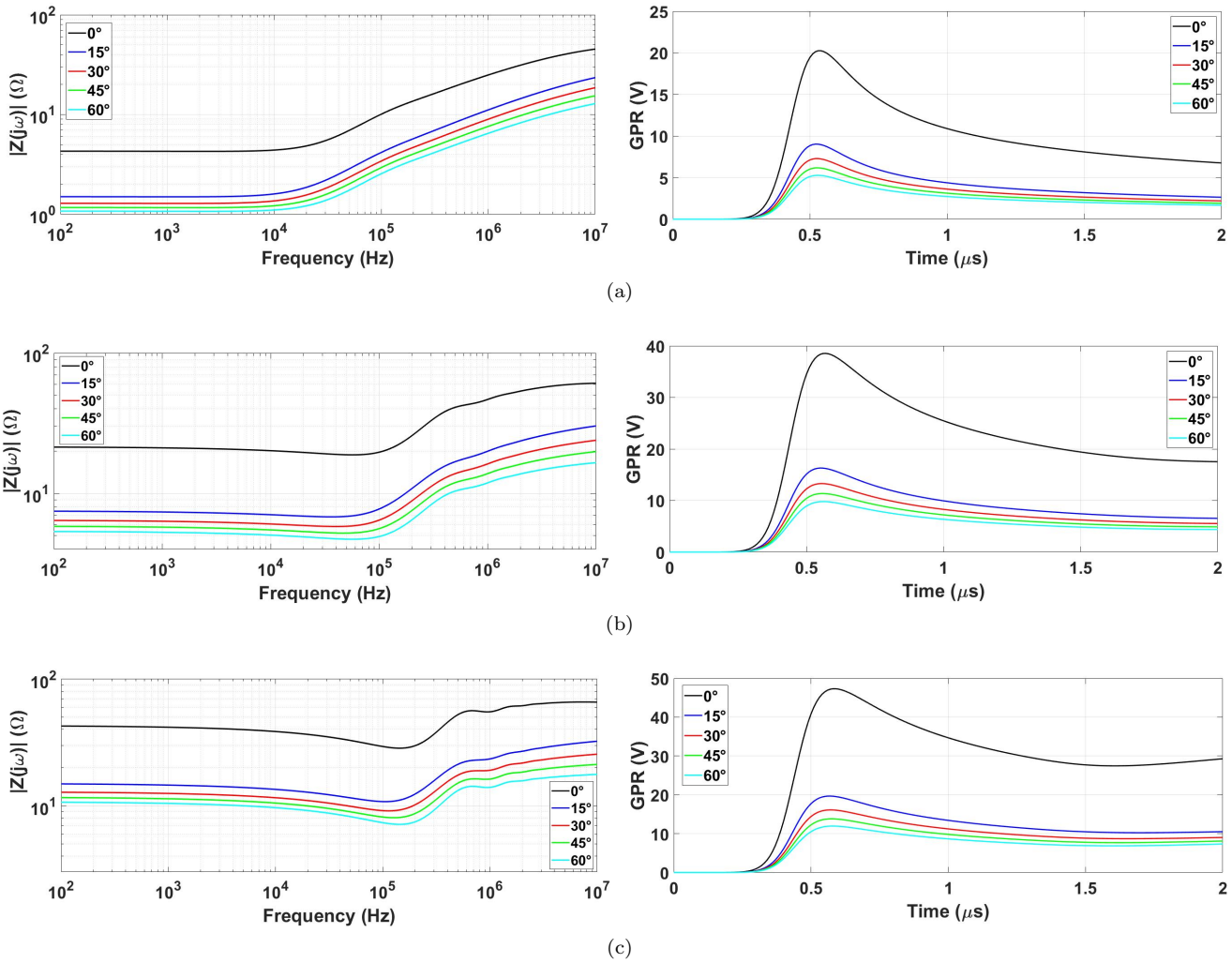

Figure 8. HGI (left) and developed GPR (right) for the topology T_4: (a) 100 Ω.m; (b) 500 Ω.m; (c) 1,000 Ω.m

GPR can be obtained exploring distinct inclination angles of the tower-footing grounding system which also tends to occupied a smaller area than the traditional grounding arrangements of long electrodes.

REFERENCES

Aniserowicz, K. (2020). Mathematical models of lightning current waveforms (pl: Modele matematyczne piorunowych udarów prądowych). *Przeglad Elektrotechniczny*, 97, 134–139.

Batista, R., Louro, P., and Paulino, J. (2021). Lightning performance of a critical path from a 230-kv transmission line with grounding composed by deep vertical electrodes. *Electric Power Systems Research*, 195, 107165.

CIGRE C4.33, W.G. (2019). Impact of soil-parameter frequency dependence on the response of grounding electrodes and on the lightning performance of electrical systems. *Tech. Brochure 781*, 1–66.

Colqui, J., de Araújo, A., de Seixas, C.M., Kurokawa, S., and Pissolato Filho, J. (2021). Performance of the recursive methods applied to compute the transient responses on grounding systems. *Electric Power Systems Research*, 196, 107281.

FEKO (2018). FEKO Altair Engineering Inc.,. URL `https://www.altair.com/feko/`.

Grcev, L. (2008). Impulse efficiency of ground electrodes. *IEEE Transactions on Power Delivery*, 24(1), 441–451.

Grcev, L., Markovski, B., and Todorovski, M. (2021). Lightning performance of multiple horizontal, vertical and inclined grounding electrodes. *IEEE Transactions on Power Delivery*, 1–1.

Grcev, L.D., Kuhar, A., Arnautovski-Toseva, V., and Markovski, B. (2018). Evaluation of high-frequency circuit models for horizontal and vertical grounding electrodes. *IEEE Transactions on Power Delivery*, 33(6), 3065–3074.

Gustavsen, B. and Semlyen, A. (1999). Rational approximation of frequency domain responses by vector fitting. *IEEE Transactions on Power Delivery*, 14(3), 1052–1061.

Usanos, E.F., Madrid, G.A., Puertas, D.G., Castejón, G.D., and Mohino, J.M. (2014). Transient behavior of a system composed of conductive thin wire structures excited by harmonic and lightning type signals. *Journal of Electromagnetic Analysis and Applications*, 6(11), 342–357.

Visacro, S. (2018). The use of the impulse impedance as a concise representation of grounding electrodes in lightning protection applications. *IEEE Transactions on Electromagnetic Compatibility*, 60(5), 1602–1605.

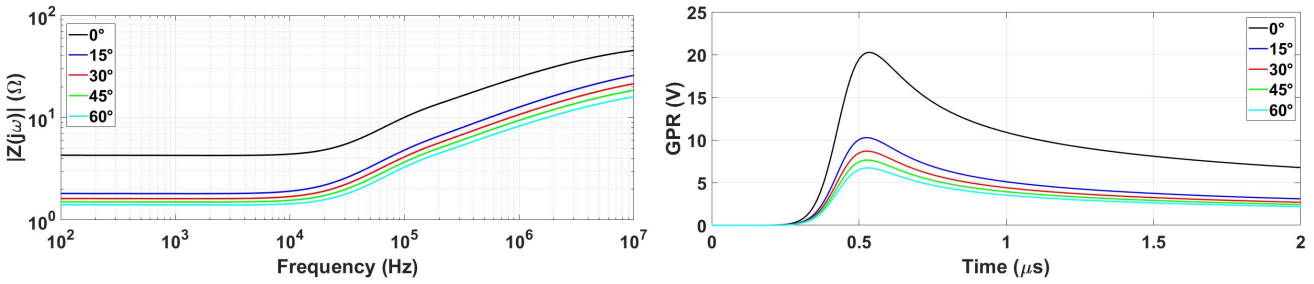

(a)

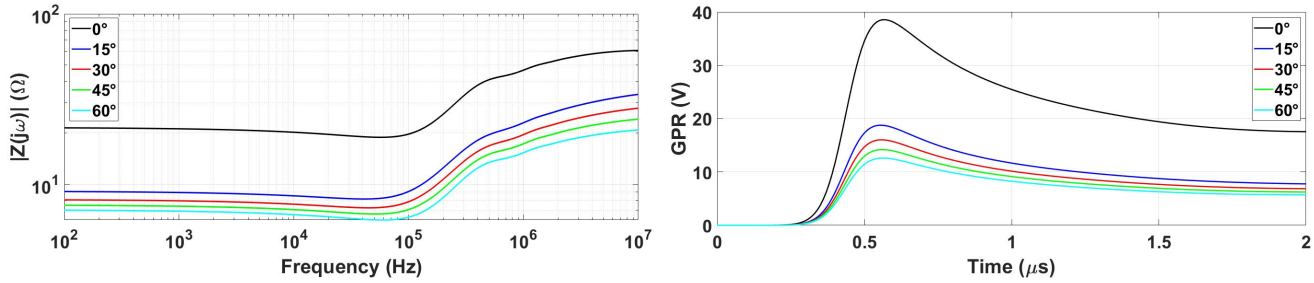

(b)

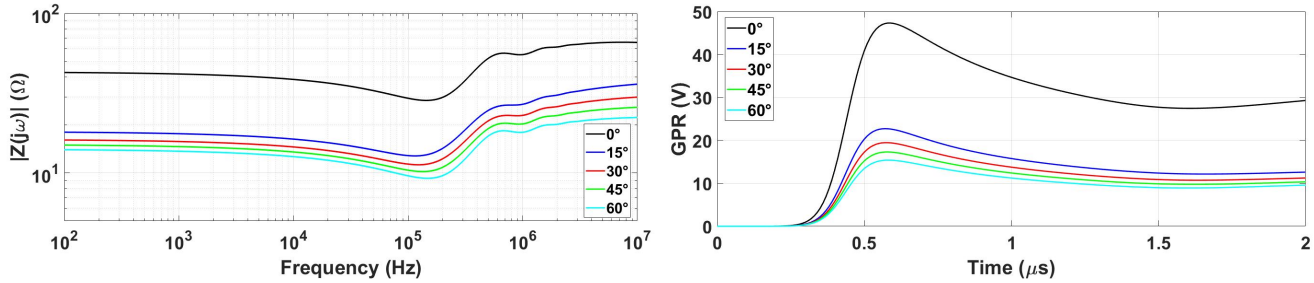

(c)

Figure 9. HGI (left) and developed GPR (right) for the topology T_3: (a) 100 Ω.m; (b) 500 Ω.m; (c) 1,000 Ω.m